

Surface plasmon laser based on metal cavity array with two different modes

Jiaqi Li,^{1,2,†} Yuan Zhang,^{1,†} Ting Mei,^{3,*} and Michael Fiddy^{4,5}

¹*Nanophotonics Lab, School of Electrical and Electronic Engineering, Nanyang Technological University, 639798, Singapore.*

²*Physics Department, Southeast University, Nanjing 211189, China*

³*Institute of Optoelectronic Materials and Technology, South China Normal University, Guangzhou 510631, China*

⁴*Center for Optoelectronics and Optical Communications, University of North Carolina at Charlotte, Charlotte NC 28223, USA*

⁵*mafiddy@uncc.edu*

**ting.mei@ieee.org*

[†] These authors contributed equally to this work

Abstract: The phenomenon of surface plasmon (SP) laser based on a square array of rectangular cavities cut into a metal substrate has been investigated. Both main resonant modes of the proposed structure can be used to realize SP laser while the working mechanism is different. We study the origin of these differences and propose an efficient design that exploits them. Besides, the effect of the sample size on SPP mode lasing is also discussed.

©2010 Optical Society of America

OCIS codes: (250.5403) Plasmonics; (310.6628) Subwavelength structures, nanostructures.

References and links

1. D. J. Bergman, and M. I. Stockman, "Surface plasmon amplification by stimulated emission of radiation: quantum generation of coherent surface plasmons in nanosystems," *Phys. Rev. Lett.* **90**(2), 027402 (2003).
2. M. I. Stockman, "Spasers explained," *Nat. Photonics* **2**(6), 327–329 (2008).
3. J. A. Gordon, and R. W. Ziolkowski, "The design and simulated performance of a coated nano-particle laser" *Opt. Expr.* **15**, 2622 (2007), <http://www.opticsinfobase.org/oe/abstract.cfm?URI=oe-15-5-2622>.
4. M. Wegener, J. L. Garcia-Pomar, C. M. Soukoulis, N. Meinzer, M. Ruther, and S. Linden, "Toy model for plasmonic metamaterial resonances coupled to two-level system gain" *Opt. Expr.* **16**, 19785 (2008), <http://www.opticsinfobase.org/oe/abstract.cfm?URI=oe-16-24-19785>.
5. Z. G. Dong, H. Liu, T. Li, Z. H. Zhu, S. M. Wang, J. X. Cao, S. N. Zhu, and X. Zhang, "Resonance amplification of left-handed transmission at optical frequencies by stimulated emission of radiation in active metamaterials" *Opt. Expr.* **16**, 20974 (2008), <http://www.opticsinfobase.org/oe/abstract.cfm?URI=oe-16-25-20974>.
6. N. I. Zheludev, S. L. Prosvirnin, N. Papasimakis, and V. A. Fedotov, "Lasing spaser," *Nat. Photonics* **2**(6), 351–354 (2008).
7. Z. G. Dong, H. Liu, T. Li, Z. H. Zhu, S. M. Wang, J. X. Cao, S. N. Zhu, and X. Zhang, "Modeling the directed transmission and reflection enhancements of the lasing surface plasmon amplification by stimulated emission of radiation in active metamaterials," *Phys. Rev. B* **80**(23), 235116 (2009).
8. M. A. Noginov, G. Zhu, A. M. Belgrave, R. Bakker, V. M. Shalaev, E. E. Narimanov, S. Stout, E. Herz, T. Suteewong, and U. Wiesner, "Demonstration of a spaser-based nanolaser," *Nature* **460**(7259), 1110–1112 (2009).
9. M. Ambati, S. H. Nam, E. Ulin-Avila, D. A. Genov, G. Bartal, and X. Zhang, "Observation of stimulated emission of surface plasmon polaritons," *Nano Lett.* **8**(11), 3998–4001 (2008).
10. A. Banerjee, R. Li, and H. Grebel, "Surface plasmon lasers with quantum dots as gain media," *Appl. Phys. Lett.* **95**(25), 251106 (2009).
11. C. P. Huang, J. Q. Li, Q. J. Wang, X. G. Yin, and Y. Y. Zhu, "Light reflection from a metal surface with subwavelength cavities," *Appl. Phys. Lett.* **93**(8), 081917 (2008).
12. C. P. Huang, Q. J. Wang, and Y. Y. Zhu, "Dual effect of surface plasmons in light transmission through perforated metal films," *Phys. Rev. B* **75**(24), 245421 (2007).
13. C. F. Klingshirn, *Semiconductor Optics*, (3rd edition, Springer, 2007).
14. M. I. Stockman, "The Spaser as a nanoscale quantum generator and ultrafast amplifier," *J. Opt.* **12**(2), 024004 (2010).

1. Introduction

In the past ten years, advances in nanotechnology have stimulated the study of Surface Plasmon Polaritons (SPPs) which have importance in many new areas. One main consequence of SPPs is that electromagnetic (EM) fields can be strongly localized and enhanced at the metal and dielectric interface. When SPPs are generated, strong interactions will occur between the EM fields and the local material properties, which can be treated as an EM cavity. By combining SPPs with gain media, Bergman and Stockman introduced the new concept of a SPASER (Surface Plasmon Amplification by Stimulated Emission of Radiation) [1,2] suggesting a new kind of laser. Recently some simulations [1,3–7] and experiments [8–10] have appeared which show that the stimulated SPP could provide a very useful source in bio-sensing. One example of the proposed SPASER [4–7] is based on a metamaterial (i.e. a periodic array of sub-wavelength elements) which shows a strong field confinement at a resonant frequency. Unfortunately, fabrication has proved an obstacle realizing such a meta-structure for visible or infrared wavelengths. This is because the unit cell of the metamaterial needs dimensions of the order of a tenth of the wavelength being employed, requiring the size of the elements in each unit cell to be even smaller. In this paper, we propose a periodic array of cavities in a metal substrate which exhibits two resonant modes. With the appropriate design, both modes can provide good field confinement that can be used to realize the surface plasmon (SP) laser phenomenon, but the working principle is different between the two modes. At visible and infrared wavelengths, comparing our design with those based on metamaterials proposed by others, ours is simpler and more straightforward to make using existing fabrication technology.

2. The structures and its passive response

A cavity array under investigation is shown in Fig. 1. It comprises cuboid cavities, arranged in a square array with lattice constant p , which are carved into a semi-infinite metal substrate and the bottoms are closed. Each cavity has dimensions of a , b and t in the x , y and z directions, respectively. The metal substrate is covered by a dielectric layer with thickness h and the background material is air. For convenience, we define the dielectric cover-layer as region I and the cavities as region II. The permittivity of the metal, the medium in the cavities, the cover-layer, and the air are denoted by ϵ_m , ϵ_{II} , ϵ_I and ϵ_0 , respectively and we adopt the Drude model to describe the metal permittivity. Linearly polarized light, with the electric field along the x direction, is incident normal to the metal surface and is reflected into the air.

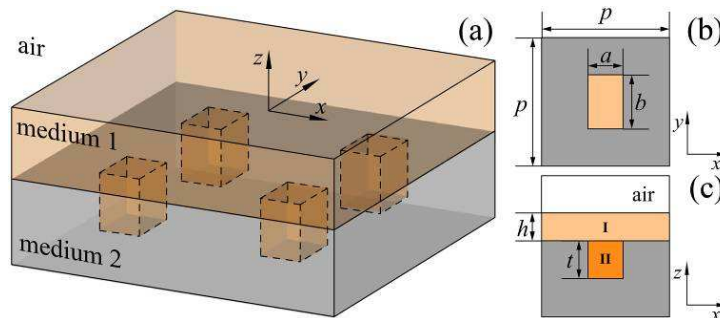


Fig. 1. (a) the schematic of our designed structure; a square array of cuboid cavities are carved into the metal substrate with a dielectric overlay, (b) the top-view and (c) the side-view of the unit cell, where $p = 1100\text{nm}$, $a = 250\text{nm}$, $b = 375\text{nm}$, $t = 500\text{nm}$, $h = 250\text{nm}$.

In order to understand the spectral response of this structure, a numerical simulation based on the full-wave finite element method was carried out. Parameters are set as: $p = 1100\text{nm}$, $a = 250\text{nm}$, $b = 375\text{nm}$, $t = 500\text{nm}$, $h = 250\text{nm}$, and $\epsilon_I = \epsilon_{II} = 2.25$, which are optimized for a high Q cavity mode and a surface mode at communication wavelength ($\sim 1550\text{nm}$). More

details of the geometry optimization can be found in Ref [11]. Besides, ϵ_m is silver having a Drude-type permittivity ($\omega_p = 1.37e16\text{rad/s}$, $\gamma = 8.85e13\text{Hz}$), and background permittivity $\epsilon_0 = 1$. The incident light has its electric field in x direction and magnetic field in y direction and we assume the ideal electric and magnetic boundary conditions are satisfied.

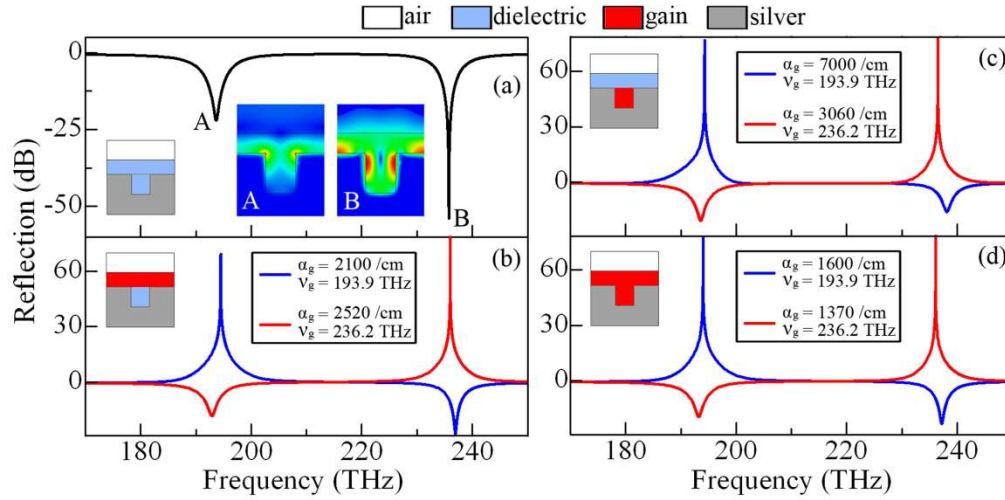


Fig. 2. The reflection spectra for normal incidence linearly polarized light on the periodic cavities for (a) the structure without gain media present and (b-d) the structure with gain media at different location as indicated in each inset. The red and blue curves represent the simulation results of gain media with different center frequencies at $\nu_g = 193.9\text{THz}$ and $\nu_g = 236.2\text{THz}$, respectively. Inset A and B in (a) show the magnetic field (H_y) distribution corresponding dip A and dip B, respectively.

The spectrum of the reflected wave is shown in Fig. 2 (a) and indicates that there are two reflection minima at around 193.9THz (A) and 236.2THz (B), which means that strong absorption occurs around those frequencies. As shown, the absorption behavior in these two regions is quite different, since dip B is much sharper and deeper than dip A. To explain the origin of this difference, we have studied the magnetic field (H_y) distribution for the two cases. As illustrated in Fig. 2 (a), inset A and inset B are the corresponding H_y distributions to dip A and dip B, respectively. It is observed that the EM fields are localized in the metal substrate surface for both dips, but there is stronger EM field in the cavity for dip B. This is in agreement with Huang's result [11] that the field of an SPP mode is partly located in region I, and partly trapped into the cavity as a Cavity Surface Plasmon (CSP) mode. Thus dip A arises from the SPP mode and dip B originates from the coupling between the SPP and the CSP modes [12]. Compared to SPP mode, the CSP mode can induce more intense field localization in the cavity leading to a lower reflection minimum. The cut-off wavelength of the cavity is a key parameter here, which can be written as [11]:

$$\lambda_c = 2\pi\sqrt{\epsilon_{11}}/(u^2 + v^2), \quad (1)$$

where, u , v are determined by $u \tan(ua/2) = -ik_0\epsilon_{11}/\sqrt{\epsilon_m}$ and $v \tan(vb/2) = -ik_0\sqrt{\epsilon_m}$, and k_0 is the wave vector in the free space. The wavelength of dip A (1546nm) is longer than the cut-off wavelength (1363nm), thus the CSP mode can't be excited and the SPP mode is the major contributor to the reflection minimum. In contrast, the SPP and CSP modes can exist simultaneously at the wavelength of dip B (1270nm , and its cutoff wavelength is 1426nm), and the CSP mode plays an important role as shown in the insets of Fig. 2 (a). Thus it can be seen that SPP mode and CSP mode play different roles in the reflection spectrum. Both modes can be used to realize an SP laser, but based on different principles, as discussed below.

3. SP laser based on different modes

The material in regions I and II can be chosen as gain media to realize SP laser. The CSP and SPP modes are surface modes, and the fields are confined to the groove dielectric/silver surface. The localized field has a strong interaction with the structure and if gain media are introduced, an efficient feedback mechanism is available. Because of the losses in the metal, there will be a threshold value of the gain media for the SP laser phenomenon. For our structure, because of the two different physical mechanisms that occur, the SPP field spreads over the surface while the CSP field is much more trapped inside the cavities and so at different locations in the gain medium, there will be different SP laser behavior.

To examine this, we set region I, region II and then region I + II to be gain media to study the effect of the location of regions of gain. The gain media considered here are dispersive, with permittivity described as [13]:

$$\varepsilon(\omega) = \varepsilon_b + \frac{\chi_0 \omega_g^2}{\omega_g^2 - \omega^2 + i\gamma_g \omega} \quad (2)$$

where ω is the angular frequency, ε_b is the background permittivity, ω_g is the resonant center angular frequency of the gain media, γ_g is the collision frequency representing the dissipation, and χ_0 is the coupling strength. For convenience, we defined the resonant frequency $\nu_g = \omega_g/2\pi$. The gain is described by the negative imaginary part of ε_b , similar to Ref [4–7], and thus the gain coefficient can be defined as:

$$\alpha = \frac{\omega}{100 \times c_0} \text{Im} \sqrt{\varepsilon(\omega)} \quad (3)$$

Here, c_0 is velocity of light in vacuum, α has units of cm^{-1} , and α_g is defined as the highest value of α and $\alpha_g = \alpha(\omega_g)$.

In the following discussion, we set $\varepsilon_b = 2.25$. We note that ε_b just determines the optical path length of the wave in the gain media, thus for different ε_b we can obtain the same simulation results by adapting the geometry of the structure to get the same optical path length. Also, $\gamma_g = 1.26 \times 10^{14}$ rad/s means a full width at half maximum (FWHM) of the gain material emission peak of $\sim 150\text{nm}$, which is reasonable for materials working at infrared wavelengths, e.g., PbS quantum dots. To study the SP laser at the two different reflection dips, the resonant frequency ν_g is taken as 193.9 THz and 236.2 THz corresponding to dip A and dip B, respectively. The gain coefficient given in Fig. 2 (b), (c) and (d) are the optimized results, and the optimization process will be discussed in the content about Fig. 3 below.

First we consider only region I is filled with the gain medium (see inset in Fig. 2(b)), while the other parameters are the same as in Fig. 2 (a). For this situation, the SPP mode on the metal surface interacts with the gain medium and the CSP mode in cavities gives a negligible contribution to the SP laser. The result (see Fig. 2 (b)) shows that for dip A ($\nu_g = 193.9$ THz), high reflection peaks of more than 60 dB can be obtained when the gain coefficient is about $\alpha_g = 2100/\text{cm}$, which means that there is strong feedback and the stimulated emission of the SPP mode takes place. For dip B ($\nu_g = 236.2$ THz), to get a high enough (>60dB) reflection peak, the required gain coefficient is around $\alpha_g = 2520/\text{cm}$ which is higher than that of dip A. The reason for this is that the reflection corresponding to dip B originates from the coupling of the SPP and CSP modes as described earlier. Consequently the interaction between the surface field and the gain medium associated with dip B is weaker than that of dip A and there is a higher gain coefficient requirement for the SP laser effect at dip B.

Secondly, the location of the gain media in the structure is changed from region I to region II (see inset in Fig. 2 (c)). This means the CSP mode is the dominant factor for the interaction between the surface field and the gain medium. Intuitively, for the reflection dip A, there is little EM field interacting with the gain medium in the cavity because its wavelength is

beyond the cut-off wavelength of the cavity. In contrast, for dip B, the EM field enters the cavities leading to the CSP mode, and a high localized EM field inside the cavities. This deduction is confirmed by our simulations shown in Fig. 2 (c). Although, high reflection peaks can be realized for both dips, we note that the gain coefficient required for dip A is much higher (α_g is about 7000/cm) than that required for dip B ($\alpha_g = 3060/\text{cm}$).

The final case is that both region I and region II are filled with the gain medium (see the inset in Fig. 2 (d)). This is a more efficient way to realize SP laser based on our structure since the SPP and CSP modes both contribute to the interaction between the surface EM field and the gain media. The calculated reflection curves are shown in Fig. 2 (d), and we can see that the gain coefficient can be quite low while still reaching a high reflection peak for both frequencies, as compared to those cases in Fig. 2 (b) and (c). We also notice that in Fig. 2 (d), the required gain coefficient is lower for dip B than that of dip A for the reasons given earlier. The EM field corresponding to dip B has longer interaction time and optical path in the gain medium and thus stronger feedback leading to better conditions for SP laser. This is also consistent with the reflection curves in Fig. 2 (a) which shows the reflection dip B is much deeper and sharper, i.e., higher Q factor for dip B than dip A. Q factor here is represented by the ratio of the center frequency and the FWHM of the resonance. The cavities are important for field localization and feedback when using the gain medium.

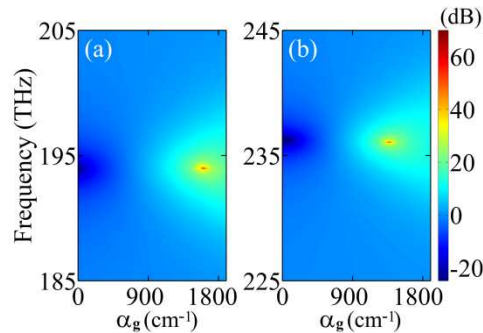


Fig. 3. (a) and (b) are calculated reflection spectra as function of α_g and frequency for dip A and dip B, respectively. Data are shown with a logarithm scale.

The SP laser reflection peaks in Fig. 2 are optimized results, that is, the peak does not continue to increase as the gain coefficient increasing. This effect in different SP laser designs has been studied and reported in Ref. 5 and 7. For the case of region I and II filled with gain media (as illustrated in Fig. 2 (d)), the relation of the reflection spectrum vs. gain coefficient has been calculated and shown in Fig. 3. The center frequency of the gain medium is still set to be $\nu_g = 193.9$ THz for dip A and $\nu_g = 236.2$ THz for dip B, and the maximum gain coefficient α_g is varied from 0 to 1800/cm. Initially, for both A and B, as the gain coefficient increases, the reflection amplitude increases to an optimum value (see those red areas in Fig. 3 (a) and (b)), and then begins to decrease if the gain coefficient keeps increasing further, which is similar to that reported in Ref. 5 and 7. In our simulation results, the width of resonance tends to be zero at the threshold of lasing and then broadens up again, owing to the fact that the gain medium is represented by an imaginary part of permittivity with negative value in this work, whereas the nature of the SP lasing as a spontaneous symmetry breaking, which leads to the establishment of the coherent SP state, is not considered [14]. Nevertheless, this simulation model is simple but useful for studying SP lasing before its lasing threshold [5–7].

The reflection peak corresponding to the SPP mode is caused by the surface periodicity, but factually, the sample should have a finite number of periods, which may limit the lasing. A sample with finite structure should be cut off along both x and y axis, but subject to the huge computational volume of a large 3D simulation, we study the problem for two separated cases, i.e. with cutoff along x and y directions respectively. The first has finite cell units in y

direction, denoted as $\infty \times n$, and the second has finite units in x , denoted as $m \times \infty$. As the electrical field is always along x direction, implying that the surface plasmon oscillation is mainly along x axis, we can expect that the cutoff in x axis will have a dominant effect on lasing as confirmed by our simulation results. A small number of units in y direction is enough for lasing in the SPP mode. An example with $n = 5$ is shown in Fig. 4 (a) and (b)

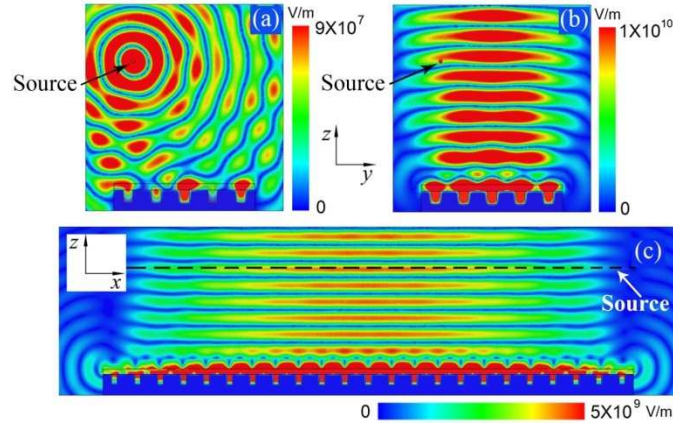


Fig. 4. Calculated E-field distribution for the SPP mode of finite array samples, (a) and (b) are corresponding to $\infty \times 5$ units array with and without gain medium, (c) $23 \times \infty$ units array with gain medium. The samples are illuminated by a line source along x -direction which are denoted by arrows.

without and with gain respectively. The calculation domain is $8\mu\text{m} \times 8\mu\text{m}$ in y - z plane and one unit cell along x -direction. The two surfaces normal to x -direction are perfect electric boundaries and the other four surfaces are absorbing boundaries (such settings ensure we are simulating $\infty \times 5$ cells). The structure is illuminated by a line source (E-field along x direction), the field around the structure in (a) is nearly two orders of magnitude smaller than that in (b). Clearly, the source pattern in (b) has been covered by the lasing beam, compared to (a). When the cutoff occurs in x direction, more units along x are needed to get an output high enough. In Fig. 4 (c), the simulation result for the case $m = 23$ (i.e. $23 \times \infty$) is shown. The calculation domain is $30\mu\text{m} \times 8\mu\text{m}$ in x - z plane, and one unit cell in y direction, the two surfaces normal to y -direction are perfect magnetic boundaries and the other four surfaces are absorbing boundaries (such settings ensure we are simulating $23 \times \infty$ cells). It is seen that the field becomes weaker towards the edges, because of periodicity breaking. This demonstrates that the amplified reflection can be realized by a sample with a finite number of periods and the sample edge scatter plays a limited adverse role.

4. Conclusion

The SP laser based on a cavity square array fabricated in a metal substrate has been studied. Both of the resonance modes of the structure can be used to realize the SP laser. By changing the gain media locations in the structure, results show that the CSP mode and SPP mode contribute quite differently when the SP laser is working at different resonant modes, which suggests that a joint contribution of CSP and SPP modes is the most efficient way to realize an SP laser. For SP laser of the SPP mode, the finite size could cause edge scattering and play negative role for lasing, but the influence can be improved when the sample contains enough units. Compared with those based on left-handed materials, this design is easier to implement using existing technology, and this work gives a new way to design an SP laser.

Acknowledgments

This work was supported by the Singapore National Research Foundation (CRP Award No. NRF-G-CRP 2007-01) and the Ministry of Education (MOE), Singapore (Research Grant No. ARC 16/07). J.Q. Li acknowledges support from the National Natural Science Foundation of China (Grant No. 10947128). T. Mei acknowledges support from Department of Education of Guangdong Province, China (Grant No. C10131).